Journal of
Materials Chemistry B

Accepted Manuscript

This article can be cited before page numbers have been issued, to do this please use: X. Hu, Y. Feng, G. Xiang, W. Lei and L. Wang, *J. Mater. Chem. B*, 2018, DOI: 10.1039/C7TB03247A.

ROYAL SOCIETY OF CHEMISTRY

rsc.li/materials-b

View Article Online
DOI: 10.1039/C7TB03247A

Journal of Materials Chemistry B

PAPER

Lactic acid of PLGA coating promotes the angiogenesis on the interface between porous titanium and diabetic bone

Received 00th January 20xx,
Accepted 00th January 20xx

DOI: 10.1039/x0xx00000x

www.rsc.org/

Xiao-Fan Hu,† Ya-Fei Feng,† Geng Xiang,† Wei lei* and Lin Wang*

The diabetes-related high failure risk for endosseous implants appeals efficacious methods to improve the osteointergration on bone-implant interface (BII). Poly (lactic-co-glycolic) acid (PLGA) is widely used in tissue engineering, but its effects on the BII in diabetes remain elusive. To clarify this issue, 3D-printed porous titanium implants (TI) with and without PLGA coating were implanted in the bone defects of sheep in vivo, and in vitro, vascular endothelial cell (VEC) and osteoblast were incubated on implant surface in normal conditions (NC) and diabetic conditions (DC). Results showed that PLGA coating promoted the angiogenesis on BII and the osteointegration of TI in diabetic sheep. PLGA coating attenuated the DC-induced dysfunctions of VEC but not of osteoblast. When VEC and osteoblast were cocultured in DC, however, PLGA coating showed protective effects on osteoblast. Lactic acid (LA) but not glycolic acid (GA), both of which are degradation products of PLGA, induced similar effects to those of PLGA. These results suggested that PLGA coating on TI could promote angiogenesis in diabetes by its degradation production, LA, thus indirectly improve the bone formation on BII. Furthermore, PLGA exerted its effects, at least partially, through inhibiting the pathological effects of advanced glycation end products (AGEs) on BII. As we know, this is the first study about the effects of PLGA on the angiogenesis on BII and the first finding about the inhibitory effects of PLGA on AGEs. Our findings prove PLGA as a promising interface-modification component for fabricating implants with better angiogenesis and osteointegration on BII under diabetic conditions. This strategy might be applicable for reducing implant failure in diabetic patients.

Introduction

Over the past few decades, with rapid increases of trauma, osteoporotic diseases, bone cancer, and joint and spinal diseases, the need for orthopedic and dental implants has undergone explosive growth, leading to growing attention on implant biomaterials.[1] Bone implants exert critical functions in medicine, but their clinical performance may dramatically decrease under some disease conditions, especially diabetes.[2, 3] Both clinical and preclinical evidence have shown that diabetic conditions (DC) led to poor bone healing at bone-implant interface (BII) and compromised implant osteointegration, resulting in a much higher failure rate of implants in diabetic patients.[4, 5] Such implant failure leads to serious complications and terrible pain for patients.[2, 3] Given that the problem takes place at BII, a special micro-environment subjected to the interaction between implant materials and the host tissue, the modification of BII might provide efficacious solutions.

Poly (lactic-co-glycolic) acid (PLGA) has attracted considerable interest as a degradable polymer for biomedical applications due to its outstanding properties such as good biocompatibility, tailored biodegradation rate and approval for clinical use by FDA and European Medicine Agency.[6] In bone tissue engineering, PLGA has been widely used in various forms: scaffolds, fibers, coatings, microspheres and so on.[7] However, despite being biocompatible, clinical application of PLGA for bone regeneration is hampered by some disadvantages like suboptimal mechanical properties for load-bearing applications.[7] Therefore, PLGA is often used in combination with other materials, such as metals and ceramics, to fabricate composite bone substitutes. When combined with metal bone implants like titanium implants (TI), PLGA could exert its functions in several possible ways, such as serving as drug-loaded component to provide controlled-release of some efficacious bioactive factors to promote the osteointegration of implants under DC. Before the possible application of PLGA as drug delivery system on BII, however, it is necessary to clarify the effects of PLGA itself on the biological responses on BII, which remain elusive, especially in the system of porous TI.

Angiogenesis, namely the formation of new blood vessels from pre-existing ones, serves as a critical component in bone healing, supplying oxygen, nutrients, stem cells and also the ions necessary for mineralization.[8] Diabetes, however, inhibits the angiogenesis in the regeneration of many tissues including bone.[9] As a degradable material, PLGA could degrade into two degradation products: lactic acid (LA) and glycolic acid (GA).[7] Although for decades LA has been merely considered as a metabolic by-product in natural organism, it is now recognized as an important contributor to angiogenesis in

Department of Orthopedics, Xijing Hospital, The Fourth Military Medical University, Xi'an 710032, P. R. China.
**E-mail: wanglinxj@fmmu.edu.cn (L. Wang), leiwei@fmmu.edu.cn (W. Lei)*
Tel: +86-029-84771011
† These authors contributed equally to this work.

View Article Online
DOI: 10.1039/C7TB03247A

wound healing for its efficacy to induce angiogenic response on vascular endothelial cell (VEC), which cell is the key executor and regulator of vascular functions.[10-12] In the study by Porporato et al., as pure LA showed weaker activity, they reported the use of PLGA as a feasible strategy to supply lactate sustainably to advance angiogenesis and wound healing.[10] However, the effects of PLGA on the angiogenesis in bone repair are still elusive, especially on the BII under diabetic conditions. Furthermore, it remains unclear about the roles of the two degradation products in the effects of PLGA on BII.

Therefore, the aims of the present study were to investigate: (1) the effects of PLGA coating of TI on the angiogenesis and bone healing at BII, especially under diabetic conditions; (2) the roles of the two degradation products of PLGA in the effects of PLGA on BII; (3) the cellular and molecular mechanisms underlying the effects of such PLGA coating.

Materials and methods

Scaffolds fabrication and surface characterization

The 3D-printed porous Ti6Al4V implants (TI) with diameter of 10 mm, height of 4 mm (Fig. 1A and B) were fabricated using electron beam melting process as previously described.[13] Briefly, the porous structure was designed with commercial CAD software (Unigraphics NX, EDS). After the CAD data of the structure was converted into STL data, imported into Materialise's Magics software, and converted into input file for EBM, the samples were produced on an Arcam's EBM machine (EBM A2, Arcam AB, Sweden).

To fabricate PLGA coating, PLGA (0.3 g, LA:GA = 50:50, molecular weight = 25000-43000, Sigma) was dissolved completely in 10 mL trichloromethane (Sigma) with a magnetic stirrer at 40℃. TI were immersed in this solution for 20 sec and then taken out for air-drying in a fume cupboard at room temperature (RT). Trichloromethane evaporated rapidly and a thin layer of reticular PLGA film was formed on the implant surface (Fig. 1C). The PLGA-coated implants are named as "PTI".

Induction of diabetic sheep model

This study was carried out strictly in accordance with the National Institutes of Health Guidelines or the Use of Laboratory Animals. The animal protocol was approved by the Fourth Military Medical University Committee on Animal Care (Approval number: FMMU-AEEA-20160903). Four adult sheep (Male, 1 year age, 60-65 kg) were subjected to the diabetic model by STZ injection as described previously.[14] Briefly, STZ (50 mg/kg) was injected into an external jugular vein for 5 consecutive days. Blood glucose level was measured every three days and the animals with serum glucose level consistently above 180 mg/dL at 3 weeks after administration were considered diabetic. In this study, all the four sheep met this standard and were used for next experiments.

Animal surgery

All the sheep were placed in quarantine for at least 7 days prior to surgery. After general anesthesia with an intramuscular injection of a mixture of Ketamine (2 mg/kg) and Diazepam (0.1 mg/kg), the sheep was fixed in right position and the hip was shaved. After the skin was sterilized with povidone-isodine solution and wrapped using sterile technique, a 10 cm longitudinal incision was made to expose crista iliaca. Four bone defects measuring Φ 10 mm × 4 mm were created with an electrical drill and then implanted (press-fit) with two TI without coating and two TI with PLGA coating. Then the surgical incision was sutured layer-by-layer. The surgical site was finally covered with an adhesive bandage. Another four TI were implanted into the crista iliaca on the other side by the same procedure. During the first week after surgery, Cephazolin (10 mg/kg) was routinely administered intramuscularly as prophylactic antibiotics once a day. 4 weeks after surgery, two normal sheep and two diabetic sheep were euthanized and the bone tissue in a ring radius 5 mm surrounding the implants were harvested from bilateral iliums for real-time quantitative PCR (qPCR) analysis of the mRNA levels of some molecules. At 12 weeks, another four animals were sacrificed and the specimens containing the implants and surrounding bone tissue were harvested for Micro-CT analysis of the bone regeneration and the osteointegration of implants.

Micro-CT analysis

Specimens were extracted (n = 6 in each group), fixed in 10% neutral buffered formalin for 5 days, placed in the sample holder and scanned under the micro-CT (eXplore Locus SP, GE Healthcare, Canada). About 1600 projections of 10242 pixels were acquired for each tomogram. The X-ray source voltage was set at 80 kV and beam current at 200 mA using filtered Bremsstrahlung radiation. The scanning angular rotation was 360°, and the angular increment was 0.40°. The projections were reconstructed using a modified parallel Feldkamp algorithm, and segmented into binary images (8-bit BMP images). For determination of the 3D micro-architectural properties within the bone regeneration area, the area of 50 pixels around the implant was selected as the region of interest (ROI). Specimens were constructed and evaluated in the ROI using 3D analysis software (Microview, GE Healthcare, Canada). The percentage of bone volume out of pore volume (BV/PV) was calculated using the threshold of 1000 for bone tissue and 4000 for implant.

Real-time Quantitative PCR (qPCR)

Bone tissue around the implants were collected at 4 weeks after surgery to evaluate the gene expressions of EMCN, CD31, VEGF-A, TGF-B1, RUNX2 and Osterix by qPCR. The total RNA in the tissue was extracted according to the instruction of RNA extract kit (Bioteck Co.). The extracted RNA samples were then reversely transcribed for the first strand cDNA synthesis, which was used to perform real-time PCR with Bio-Rad CFX Manager system. The primers used in this study were listed in Table 1 and β-actin was used as a housekeeping gene.

Cell culture on implants

Human Umbilical Vein Endothelial Cells (HUVEC) was purchased from American type culture collection (ATCC). Primary rat osteoblasts were isolated from calvaria of neonatal Sprague-Dawley Rats with the enzymatic isolation method as previously described.[15]

View Article Online
DOI: 10.1039/C7TB03247A

Both cells were cultured in Dulbecco's modified Eagle's medium (DMEM, Gibco) supplemented with 10% fatal bovine serum (FBS), 1% penicillin and streptomycin. HUVECs at passages between 4 and 7 and osteoblasts at passages between 2 and 4 were used in all experiments to be seeded on the specimens with 1 × 104 cells/ml and randomized to incubate with normal conditions (NC) or diabetic conditions (DC) in 24-well plates with 2 ml culture media in each well. The culture media were changed every other day. These two cells were cultured on implants alone or co-cultured by Transwell system (Fig. 6C). DMEM containing 25 μmol/L glucose and 500 μmol/L BSA-conjugated palmitate (high glucose and fat) was used as the mimic conditions of diabetes and labeled as ''DC".[16] Additional drugs, namely lactic acid (LA, 112.3 μmol/L, Sigma), glycolic acid (GA, 166.3 μmol/L, Sigma), aminoguanidine (Ami, 500 μmol/L, Selleckchem) and AGE (AGE-BSA, 100 μg/ml, please see the method subsection "Preparation of AGE"), were added into the culture media according to the experimental groups. The concentrations of LA and GA were determined as the average concentrations of these two substances detected in the first 6 days of PLGA degradation experiments (Fig. 7). And the concentrations of aminoguanidine[17] and AGE-BSA[18] were chosen according to previous studies.

Co-culture of VEC and osteoblasts on implants was conducted in Transwell system, as shown in Fig. 6C. HUEVC on implants were incubated in the lower chamber and osteoblasts on the same implant were cultured in the upper chamber, without direct contact between these two cells.

Cell proliferation and adhesion

After 7 days of incubation, cell proliferation was assessed using methylthiazol tetrazolium (MTT) assay and immunoflurescent staining of Ki-67, a cell proliferation marker, as previously described.[19, 20] The cell viability in MTT assay was expressed as the absorbance per gram of sample. To evaluate cell adhesion and morphology, cellular actin filaments and nucleus were visualized respectively by staining with Alexa Fluor® 488 Phalloidin (Cell Signaling Technologyy, Beverly, MA, USA) and 40, 60-diamidino-2-phenylindole (DAPI, Sigma, St. Louis, MO) as we reported previously.[15] Briefly, the samples were fixed with 4.0% paraformaldehyde for 10 min and permeabilized with 0.1% Triton X-100 for 3 min, respectively. After blocking non-specific antibody binding with 1.0% BSA for 20 min, the samples were incubated with rat anti-Ki-67 primary antibody in PBS overnight at 4°C. After washing for 3 times with PBS, the samples were incubated with Alexa Fluor® 594 donkey anti-rat secondary antibody at room temperature (RT) for 1 h. Then the samples were further stained with Alexa Fluor® 488 Phalloidin and DAPI for 15 min at RT. The samples were then mounted and fluorescence images were obtained by a laser scanning confocal microscope (The Olympus Fluoview). The percentage of Ki-67+ cells, the cell area and cell density were measured using the Image J software package. Six different substrate fields were measured per sample, and three separate samples were measured in each group.

Angiogenesis in vitro by tube formation test

A Matrigel tube-formation assay was performed to assess in vitro angiogenesis.[21] 7 days after incubation, VEC on the implants were trypsinized with 0.05% pancreatic enzyme, resuspended at 2×10^5 cells/mL with culture media containing 1% FBS and plated at 2×10^4 cells/well in 96-well plates precoated with growth factor-reduced Matrigel (BD, San Jose, CA, USA). After 5 - 6 hours, the tube formation by VEC on Matrigel surface was observed with microscope (Zeiss). Pictures in five fields were captured and counted for each well, with three wells detected for each group. The mean tube length per field was quantified by Image-Pro Plus 6.0 software.

Cell migration assessed by wound-healing assay

Wound-healing assay was performed as previously described with some adjustment.[22] 7 days after incubation, VEC on the implants in different groups were trypsinized, resuspended in DMEM containing 5% FBS, plated in 48-well plates at 2×10^5 cells/well and cultured for 12 h to form confluent cell monolayer in the wells. Confluent monolayers were serum starved for 2 h and then were wounded with a pipette tip. After three washes to remove the detached cells, the remaining cells were incubated in serum-starved medium. The area of the cell-free wound was recorded in four fields in each well using microscope (Axiovert D1; Zeiss) immediately (0 h) after wounding. 12 h later, pictures were taken at the same places and the area of the cell-free wound was recorded again. The captured images were analyzed using Image J software. The percentage of healing was calculated by subtracting the area of the wound at 12 h from the initial wound area at 0 h.

Enzyme-Linked Immunosorbent Assay (ELISA)

7 days after incubation, ELISA kits (R&D Systems, Minneapolis, MN, USA) were used to determine the levels of cytokines, namely VEGF-A (Catalog-DVE00) and TGF-B1 (Catalog-DB100B), in cell culture supernatant according to manufacturer's instructions. Data were measured with a microplate reader and reported as pg/ml or ng/ml. The levels of two representative AGEs, pentosidine (Catalog-LS-F24997) and Nε-carboxymethyllysine (CML, Catalog-LS-F27668) in the VEC were also detected with ELISA kits (LifeSpan BioSciences, USA), normalized by protein content and reported as ng/mg protein.

Osteogenic differentiation of osteoblasts

To evaluate osteoblast differentiation in early phase, alkaline phosphatase (ALP) activity was measured with p-nitro-phenyl phosphate (p-NPP) as substrate after 7 days of incubation.[15] The optical density of p-nitrophenol formed was measured on a spectrophotometer at 405 nm. The protein concentration was determined by a micro-BCA assay kit (Beyotime, China), and ALP activity was normalized to the total protein concentration and expressed as μmol/h/mg protein.

Determination of the concentrations of LA and GA

The degradation of PLGA coating with time was evaluated both when incubated with VECs and when immersed in PBS (pH 7.4) with equal volume to the culture media in each well. The concentrations of the two degradation products of PLGA, LA and GA, in the media were measured using high-performance liquid chromatography (HPLC).[22] At predetermined time points, the PBS or culture

View Article Online
DOI: 10.1039/C7TB03247A

supernatant containing degradation products was used for HPLC. For the degradation in PBS, different paralleled experiments independent to each other were done for different time points. For the degradation with cells, the supernatant detected were those removed from the culture plates for culture media replacement every two days. In HPLC, 1 ml of the liquid was centrifuged at 12000 rpm for 15 min and the supernatant were filtered through a 0.22 μm membrane filter. A volume of 20 μl sample was injected into the HPLC (Shimadzu LC-10AS Liquid Chromatography, Japan) using organic column packed with 9 μm polystyrene divinylbenzene ion exchange resin (Aminex HPX-87H; Bio-Rad Laboratories, USA). The column was operated at 65°C, flow rate of 0.7 ml/min, mobile phase (0.009 N sulphuric acid), and a UV detector of λ 220 nm which was determined from the preliminary scanning of best absorbance wavelength. The concentrations of LA and GA were determined by integrating the peak areas with a calibration curve of standard solutions of LA and GA.

Determination of the levels of advanced glycation end products (AGEs) and receptor for AGEs (RAGE)

7 days after incubation, the levels of AGEs and RAGE in VEC on implants were determined. ELISA kits (LifeSpan BioSciences) were used to determine the levels of two representative AGEs, pentosidine and CML. Briefly, cell media were removed and cells on implants were washed 3 times with 0.1 M PBS. After lysed in 1 ml RIPA buffer on ice for 10 min, the cell lysates were tested by ELISA assay. Protein levels of RAGE in cells were detected by Western blotting analysis with a goat anti-RAGE primary antibody (R&D Systems) as previously described[14] and normalized to the levels of β-actin.

Preparation of AGE

AGE was obtained by long-term exposure of albumin (BSA) to glucose.[23] BSA at 50 mg/ml (low endotoxin, fatty acid free; Sigma) was incubated with 0.5 mol/L glucose in PBS (pH 7.4) containing protease inhibitors and antibiotics at 37°C for 6 weeks under aseptic conditions to form AGE-BSA. Control proteins were exposed to 37°C for the same time interval and in the same buffer, except for the absence of glucose. The unincorporated sugars were removed utilizing dialysis against PBS. Endotoxin levels were checked using an endotoxin testing kit (Limulus J Single Test, Wako Pure Chemical Industries, Osaka, Japan). AGE-BSA solution at the concentration used for cell culture in this study, 100 μg/ml, was confirmed to be endotoxin free (< 2.5 U/ml of endotoxin).

Statistical analysis

The results were presented as the means ± SEM for each group of at least three independent experiments with duplicate sample. A one-way ANOVA followed by Bonferroni's multiple comparison test was used for statistical analysis. $P < 0.05$ was considered statistically significant.

Results

The effects of PLGA coating on the osteointegration of TI

It has been reported that PLGA coating on TI just could induce insignificant effects on the implant osteointegration in normal conditions (NC).[24] And the main aim of the present study was to see whether PLGA coating could help to reduce the implant failure in diabetic patients. Thus, in our study design, PLGA-coated TI (PTI) were tested only under diabetic conditions (DC) to find out whether PLGA coating could improve the osteointegration of TI under DC and the underlying mechanism. The environment in vivo is much more complicated than that in vitro, and the effectiveness of a therapeutic strategy could be meaningful for clinical application only if it has been verified in vivo. Thus, to evaluate the effects of PLGA coating on the bone regeneration on BII, we firstly conducted experiments in vivo: TI without coating and PTI were implanted in the ilia of sheep, with Micro-CT analysis conducted at 12 weeks post-operation (Fig. 2). Reconstructed 3D stereoscopic pictures of implants and bone tissue showed the new bone ingrowth into the implant pores. For TI without coating, in NC, the host bone tissue (yellow) was observed to grow into the implants (cyan) from the margin into the center. In DC, however, the new bone formation was detected only in the peripheral region of implants. Quantitative analysis of the bone ingrowth within the whole implant was done with the ratio of bone volume to pore volume (BV/PV). For non-coated TI, the BV/PV in DC was significantly lower than that in NC (DC+TI group *vs*. NC+TI group, 8.3 ± 1.31% *vs*. 28.5 ± 2.88%, $p < 0.05$). Compared with non-coated TI, PTI induced obviously better new bone ingrowth and significantly higher BV/PV (18.4 ± 3.02%, $p < 0.05$) in diabetic animals (DC+PTI group *vs*. DC+TI group).

The effects of PLGA coating on the functions of VEC and osteoblast in the tissue around TI

After making clear the effects of PLGA coating on the osteointegration of TI, we wanted to know the mechanisms underlying such effects. In bone repair, VEC is the key cell in angiogenesis and osteoblast is the key cell for osteogenesis. To investigate why PLGA coating promoted the osteointegration of TI under DC, we evaluated the status of these two cells in the tissue around implants at 4 weeks by qPCR analysis of the expressions of some critical molecules (Fig. 3). The levels of two key transgenic factors expressed specifically in osteoblasts during osteogenic differentiation, namely RUNX2 and Osterix, and two VEC markers, EMCN and CD31, showed the amount of osteoblasts and VECs in the tissue. The levels of 3 representative cytokines crucial for both angiogenesis and osteogenesis, namely VEGF-A and TGF-B1, were also determined to assess the cellular secretory function and the communication among these cells. The results showed that, in the tissue around TI, DC led to markedly lower levels of all the molecules as compared with those in NC. PLGA coating induced significant increase in the molecular expressions in DC (DC+PTI group *vs*. DC+TI group).

The effects of PLGA coating on the behaviours of VEC and osteoblast on TI surface in vitro

As aforementioned, the biological environment in vivo is complicated. So the effects of PTI on the osteoblast and VEC on BII could be direct or indirect. To directly evaluate the effects of PLGA

View Article Online
DOI: 10.1039/C7TB03247A

coating on VEC and osteoblast, HUVEC and primary rat osteoblast were cultured on different implants, and the cell behaviours in different conditions were assessed 7 days after incubation. For VEC, we evaluated cell proliferation by MTT assay (Fig. 4A) and immunofluorescent staining of Ki-67 (a cell proliferation marker, Fig. 4A and C), cell adhesion by cytoskeleton staining (Fig. 4A), cell area (Fig. 4D) and cell density (Fig. 4E). In addition, the in vitro angiogenesis of VEC was evaluated by tube formation test (Fig. 5A-C), with cell migration tested by wound-healing assay (Fig. 5D and E). Compared with NC, DC induced significant inhibition on all the tested functions of VEC on implant surface. However, in DC, VEC on PLGA-coated implants showed obviously better cell functions, evidenced by higher cell proliferation, better cell adhesion and angiogenesis in vitro (more tube formation) as well as increased cell migration (DC+PTI group *vs*. DC+TI group).

For osteoblast, we tested cell proliferation by MTT assay and osteogenic differentiation by colorimetric assay of intracellular ALP activity at day 7 (Fig. 6). When osteoblast was culture alone on implants, compared with NC, DC induced obvious dysfunctions of osteoblast (Fig. 6A and B). Remarkably, in DC, the behaviors of osteoblast on PTI were similar to those on TI. Interestingly, when osteoblast and VEC were cocultured in Transwell system in DC (Fig. 6C), osteoblast showed significantly higher proliferation (Fig. 6D) and better osteogenic differentiation (Fig. 6E) on PTI than on TI. In addition, the levels of two cytokines critical for both angiogenesis and osteogenesis in the culture supernatant also showed similar changes in the co-culture system (Fig. 6F and G).

The degradation of PLGA coating

The differences between PTI and TI were two things: the existence of PLGA coating and the interaction between PLGA and Ti. As a well-known degradable material, PLGA could degrade into two products, LA and GA. In previous studies, PLGA itself was reported to induce accelerated angiogenesis in skin wound healing, which effects were explained to be mainly related to the capability of LA in promoting angiogenesis.[10] So we next studied the roles of these two degradation products in the effects of PLGA coating on BII. Firstly, the degradation of PLGA coating was evaluated in two different environments: when immersed in PBS and when incubated with VEC. Surface characteristics of the implants were observed with SEM (Fig. 7A) and the concentrations of the two degradation products in the media were measured using HPLC (Fig. 7B). In PBS without cells, the reticular PLGA coating showed slight degradation on day 2 but obvious degradation on day 7 with squamaceous coating residue on titanium surface (Fig. 7A). The concentrations of LA and GA in PBS showed sustained growth in the first 10 days, but the growing speed decreased after day 6, which was consistent with the SEM results showing that most of the coating had already degraded on day 7. When the coated implants were incubated with VEC, the existence of cells led to obvious degradation of PLGA coating on day 2 and, on day 7, only cells could be seen on the titanium surface with no observable coating. In line with this cell-induced speed-up of coating degradation, on day 2, the concentrations of the two degradation products in culture supernatant were higher than those in PBS. With the regular replacement of culture media every two days, the concentrations of LA and GA in supernatant decreased on day 4 and day 6. Given that the monomer proportion of PLGA used here was 50:50, the obvious lower concentration of LA than that of GA in culture supernatant might be related to the cell activities. In addition, with the degradation of PLGA, the pH in PBS decreased slowly, while the pH in culture supernatant kept relatively stable near 7.3 (Fig. 7C). The pH in supernatant declined on day 2 and rose again on day 4 and 6, which were consistent with the concentration changes of the degradation products.

The effects of LA and GA on the VEC on TI surface in diabetic conditions

Next, the roles of the two degradation products was evaluated by adding LA (112.3 μmol/L) or GA (166.3 μmol/L), to the culture media for VEC on TI and testing the cell behaviours (Fig. 8). 112.3 μmol/L is the mean value of LA concentration in the culture supernatant on day 2 to day 6 in the coating degradation experiments (Fig. 7B), and 166.3 μmol/L is that of GA. Results showed that, in DC, LA promoted the functions of VEC in adhesion (Fig. 8A and B, DC+TI+LA group *vs*. DC+TI group), proliferation (Fig. 8C-E), migration (Fig. 8H and I) and angiogenesis in vitro (Fig. 8F and G), which effects were similar to those from PLGA. GA, however, only made insignificant influence on the behaviors of VEC in DC (DC+TI+GA group *vs*. DC+TI group). Next, the effects of LA at different concentrations (100, 500 and 2500 μM) on the proliferation of VEC on TI in DC were examined (Fig. 8D). Interestingly, only the relatively lower two doses of LA promoted VEC proliferation, while the higher dose at 2500 μM induced mild inhibition on cell proliferation.

The effects of PLGA coating on the formation and effects of advanced glycation end products (AGEs) in VEC

Next, there came the question what was the mechanism underlying the effects of PLGA on VEC in DC. Considering the role of AGEs as an accessary in diabetes-induced angiogenesis inhibition and diabetic bone complications,[18, 25] we further investigated the relationship between AGEs and the effects of PLGA.

Firstly, the levels of AGEs and receptor for AGEs (RAGE) in VEC under different conditions were determined by ELISA assay and Western blot analysis respectively (Fig. 9). Compared with NC, DC led to prominent increase of two representative AGEs, pentosidine and CML, as well as RAGE in the VEC on TI (DC+TI group *vs*. NC+TI group). These DC-induced changes were significantly inhibited by the existence of PLGA coating (DC+PTI group). LA at 112.3 μM made effects similar to those by PLGA, while GA only slightly reduced the AGEs and RAGE in VEC on implants.

Aminoguanidine (Ami), an inhibitor of AGEs formation,[17] significantly reduced the levels of both AGEs and RAGE in VEC in DC (Fig. 11) and showed similar beneficial effects on VEC to those by PLGA coating (DC+TI+Ami group, Fig. 10). In NC, the addition of AGE (AGE-conjugated BSA) caused obvious dysfunction of VEC on TI

View Article Online
DOI: 10.1039/C7TB03247A

(NC+TI+AGE group *vs*. NC+TI group, Fig. 10), which was significantly attenuated by PTI (NC+AGE+PTI group). The AGE-induced up-regulation of both AGEs and RAGE in the VEC in NC were also significantly inhibited by PLGA coating (Fig. 11).

Discussion

The serious consequences of diabetes-induced bone implant failure require efficacious strategies to promote the osteointegration at bone-implant interface (BII). In the present study, the main findings were as follows: First, reticular PLGA coating on the surface of 3D-printed porous titanium implant (TI) attenuated the diabetes-induced poor bone regeneration on BII and improved the implant osteointegration. Second, the PLGA-induced promotion on bone regeneration was mainly exerted by attenuating the diabetes-induced inhibition on the VEC and angiogenesis on BII. Third, the effects of PLGA coating were mainly mediated by one of its degradation products, lactic acid (LA) but not glycolic acid (GA). Forth, the beneficial effects of PLGA on VEC were closely related to inhibiting the pathological effects of AGEs under diabetic conditions.

PLGA has been widely and clinically applied in bone substitutes, but its effects on the bone healing in DC remain elusive, especially at BII. Two previous reports showed that drug-containing PLGA microsphere on TI surface effectively promoted the implant osteointegration in diabetic animals,[26, 27] but neither of them evaluated the effects of PLGA itself. In the present study, PLGA coating on the 3D-printed porous TI effectively promoted the bone ingrowth of implants in diabetic animals. This is inconsistent with Liu, et al reporting that PLGA sheet on the surface of oral TI made no difference on the implant osteointegration in diabetic rats.[28] This discrepancy may be related to that, compared with the study by Liu, et al, (1) the 3D-printed porous architecture of TI in our study induced different biomechanical environment and biological process at BII;[29, 30] (2) the larger surface area of porous implant and the reticular structure of PLGA coating led to different degradation kinetic of PLGA,[31] leading to different concentration of LA in local tissues, while our results showed that the effects of LA on the VEC on TI were dose-dependent (Fig. 8D). Actually, our results are in line with another report showing that PLGA microsphere itself promoted the skin wound healing in diabetic animals.[32] These together suggested that PLGA might be an excellent interface-modification component to fabricate composited implant materials with better osteointegration under diabetic conditions. Specifically, thin and reticular PLGA coating on porous TI may help to reduce implant failure in diabetic patients. Such PLGA coating could be loaded with other effective constituents like bioactive factors to further the bone healing on BII.

In bone repair, osteoblast is the direct executor of bone formation, and blood vessel is the key transport corridor of crucial elements for tissue regeneration, such as cells, nutrients and bioactive factors.[8] In the present study, quantitative analysis of some key markers in the tissue around implants (Fig. 3) showed that PLGA coating significantly attenuated the diabetes-induced inhibition on both the angiogenesis and osteogenesis at BII. In results in vitro, however, PLGA coating attenuated the DC-induced dysfunction of VEC but not of osteoblast on TI. When VEC and osteoblast were cocultured, PTI induced increase of cytokines in the culture supernatant (Fig. 6F and G) and the bio-functional recovery of osteoblasts in DC (Fig. 6D and E). Recently, collective evidence show that the importance of organ-specific VEC lies not only in their role as a crucial part of blood vessels, but also in their role as an indispensable regulator of other local cells through cell-to-cell cross-talking by cytokines like VEGF-A.[33, 34] Our results are consistent with previous studies showing that, compared with monoculture, coculture of VEC and osteoblast led to obviously better cell functions of both of these two cells.[35, 36] All these together suggest that the facilitative effects of PLGA coating on osteoblast in vivo (Fig. 3E and F) might not be direct. Instead, PLGA directly promoted the functions of VEC which exerts substantial supports for osteogenic cells through mechanisms including intercellular communication by cytokines, and thus indirectly mitigated the DC-induced dysfunction of osteoblast. In another words, it was the enhanced functions of VEC and accelerated angiogenesis on BII that contributed more to the improved bone ingrowth in PTI in diabetic animals.

As a well-known degradable polymer, PLGA can degrade into LA and GA.[10, 11, 32, 37] In the present study, LA, rather than GA, made positive effects similar to those of PLGA coating (Fig. 8), suggesting that the effects of PLGA coating were mainly mediated by one of its degradation products, LA. This also suggested that the improved osteointegration in vivo by PTI might be correlated mainly with PLGA itself. The fact that the effects of PLGA coating were detected in the tissue not directly contacted with the implants (Fig. 3) further suggested that PLGA exerted chemical influence at the BII through releasing LA. These are consistent with previous studies showing that LA serves as an important mediator of angiogenesis in wound healing [10, 12] and tumor growth.[37] Of course, however, we can't exclude the possibility that the interaction between Ti and PLGA might also be involved in the beneficial effects of PTI. In our results, LA showed concentration-dependent effects on the VEC on implants (Fig. 8D), with slightly passive influence on VEC at 2.5 mM, a relatively higher concentration. This is in line with the fact that the LA level in normal physiological conditions is ~1.8 mM[38] and the report from Florent, et al[39] showing that LA at concentrations higher than 3 mM could be harmful to osteoblast. Such concentration-dependent effects of LA may be related to the different results about the effects of PLGA coating on implant osteointegration as mentioned above. So, in composite material design in the future, the amount, shape and monomers' ratio of PLGA need to be optimized to provide proper concentration of LA in local tissues, performing the proangiogenic function of LA and avoiding its negative effects at high concentrations.

AGEs are end products of non-enzymatic glycosylation reactions between reducing sugars and other biomolecules, such as proteins, lipids or nucleic acids.[18] They exist both inside and outside of cells,

View Article Online
DOI: 10.1039/C7TB03247A

and exert effects through receptor binding as well as intracellular signaling.[18] AGEs are formed throughout life, but in low level and cleared from our body in time.[25] During aging and many diseases, such as neurodegenerative diseases, nephropathy, osteoarthritis and especially diabetes, the formation and deposition of AGEs greatly accelerate in many tissues, impacting extracellular and intracellular structure and function.[18] AGEs have been shown to be a substantial contributor to a variety of diabetic complications, especially vascular injury[25] and impaired angiogenesis,[40, 41] through engaging the receptor for AGEs (RAGE) to induce intracellular metabolic abnormalities and by the formation of cross-links between molecules in extracellular matrix. As for bone, both clinical and preclinical studies have shown that there is much higher accumulation of AGEs in bone in diabetes. The excess of AGEs leads to abnormalities of bone cells and cross-linking of organic bone matrix, adversely affecting the quality of bone material and the fracture resistance of bone.[42-44] In addition, it has been proposed that the AGEs-related vascular calcification might be an important contributor to diabetic osteopenia. [45]

Given the vicious character of AGEs in many diseases, they have been the subject of ongoing research as important therapeutic targets through three main approaches: (1) preventing the formation of AGEs with drugs like aminoguanidine (Ami); (2) breaking crosslinks after they are formed and (3) preventing their negative effects through reducing RAGE or blocking the interaction between AGEs and RAGE with agents like sRAGE, a decoy receptor for AGEs.[18, 25] In the present study, DC led to obvious increase of AGEs and RAGE in VEC on TI, while both PLGA coating and LA effectively inhibited these changes. Aminoguanidine, an inhibitor for AGEs formation, showed similar beneficial effects to those by PLGA. In addition, AGE alone caused dysfunction of VEC on TI in NC, which was significantly attenuated by PTI. These together suggest that the diabetes-induced angiogenesis impairment at BII are closely related to AGEs, while PLGA exerts its effects on angiogenesis and bone regeneration, at least partially, through interfering with the intracellular formation of AGEs and inhibiting the effects of AGEs by reducing RAGE. As far as we know, this is the first finding about the effects of PLGA and LA on AGEs-related pathological mechanisms. Provided that AGEs are implicated in various tissue failure in many chronic diseases, such efficacy of PLGA might make it a promising biomaterial for tissue regeneration under many disease conditions, especially for bone regeneration under diabetic conditions.

Conclusions

PLGA-coating on porous titanium implants could promote the angiogenesis at the bone-implant interface (BII) under diabetic conditions by releasing degradation product, lactic acid (LA), and thus indirectly improve the osteogenesis and the osteointegration of implants. PLGA coating exerts its beneficial effects on the angiogenesis at BII, at least partially, through inhibiting the diabetes-induced formation of AGEs in VEC and attenuating the pathological effects of AGEs on VEC by down-regulating RAGE. Given that angiogenesis plays a critical role in tissue regeneration and PLGA is one of the few polymers approved for clinical use in humans, our findings prove PLGA as a recommendable interface-modification component in implant fabrication to promote the angiogenesis on material-tissue interface. Specifically, producing porous metal implants with reticular PLGA coating to obtain better angiogenesis and osteointegration at BII might be an applicable strategy to reduce implant failure in diabetic patients.

Conflicts of interest

There are no conflicts of interest to declare.

Acknowledgements

This work was supported by the Research Fund for the National Natural Science Foundation of China to Lin Wang (No. 81371933), to Ya-Fei Feng (No. 81401769) and to Wei Lei (No. 81672132). The authors acknowledge the technical support from the School of Mechanical Engineering, Shanghai Jiao Tong University, China.

References

1. X. Lin, S. Yang, K. Lai, H. Yang, T. J. Webster and L. Yang, *Nanomedicine : nanotechnology, biology, and medicine*, 2017, **13**, 123-142.
2. B. R. Chrcanovic, T. Albrektsson and A. Wennerberg, *Journal of dental research*, 2014, **93**, 859-867.
3. V. Moraschini, E. S. Barboza and G. A. Peixoto, *International journal of oral and maxillofacial surgery*, 2016, **45**, 1237-1245.
4. S. Annibali, N. Pranno, M. P. Cristalli, G. La Monaca and A. Polimeni, *Implant dentistry*, 2016, **25**, 663-674.
5. N. N. Le, M. B. Rose, H. Levinson and B. Klitzman, *Journal of diabetes science and technology*, 2011, **5**, 605-618.
6. F. Danhier, E. Ansorena, J. M. Silva, R. Coco, A. Le Breton and V. Preat, *Journal of controlled release : official journal of the Controlled Release Society*, 2012, **161**, 505-522.
7. P. Gentile, V. Chiono, I. Carmagnola and P. V. Hatton, *International journal of molecular sciences*, 2014, **15**, 3640-3659.
8. S. Stegen, N. van Gastel and G. Carmeliet, *Bone*, 2015, **70**, 19-27.
9. J. A. Beckman and M. A. Creager, *Circulation research*, 2016, **118**, 1771-1785.
10. P. E. Porporato, V. L. Payen, C. J. De Saedeleer, V. Preat, J. P. Thissen, O. Feron and P. Sonveaux, *Angiogenesis*, 2012, **15**, 581-592.
11. F. Vegran, R. Boidot, C. Michiels, P. Sonveaux and O. Feron, *Cancer research*, 2011, **71**, 2550-2560.
12. K. K. Chereddy, R. Coco, P. B. Memvanga, B. Ucakar, A. des Rieux, G. Vandermeulen and V. Preat, *Journal of controlled release : official journal of the Controlled Release Society*, 2013, **171**, 208-215.
13. Y. F. Feng, L. Wang, Y. Zhang, X. Li, Z. S. Ma, J. W. Zou, W. Lei and Z. Y. Zhang, *Biomaterials*, 2013, **34**, 2234-2243.
14. X. Li, X. Y. Ma, Y. F. Feng, Z. S. Ma, J. Wang, T. C. Ma, W. Qi, W. Lei and L. Wang, *Biomaterials*, 2015, **36**, 44-54.
15. X. F. Hu, L. Wang, Y. Z. Lu, G. Xiang, Z. X. Wu, Y. B. Yan, Y. Zhang, X. Zhao, Y. Zang, L. Shi, W. Lei and Y. F. Feng, *Acta biomaterialia*, 2017, **61**, 233-248.

View Article Online
DOI: 10.1039/C7TB03247A

16.X. Tong, T. Kono, E. K. Anderson-Baucum, W. Yamamoto, P. Gilon, D. Lebeche, R. N. Day, G. E. Shull and C. Evans-Molina, *Diabetes*, 2016, **65**, 3039-3052.
17.B. Duran-Jimenez, D. Dobler, S. Moffatt, N. Rabbani, C. H. Streuli, P. J. Thornalley, D. R. Tomlinson and N. J. Gardiner, *Diabetes*, 2009, **58**, 2893-2903.
18.C. Ott, K. Jacobs, E. Haucke, A. Navarrete Santos, T. Grune and A. Simm, *Redox biology*, 2014, **2**, 411-429.
19.X. Y. Ma, Y. F. Feng, Z. S. Ma, X. Li, J. Wang, L. Wang and W. Lei, *Biomaterials*, 2014, **35**, 7259-7270.
20.L. M. Hassman, T. J. Ellison and D. H. Kedes, *The Journal of clinical investigation*, 2011, **121**, 752-768.
21.X. Hu, L. Zhang, J. Jin, W. Zhu, Y. Xu, Y. Wu, Y. Wang, H. Chen, K. A. Webster, H. Chen, H. Yu and J. Wang, *Stem cells*, 2015, **33**, 1850-1862.
22.P. Outeda, D. L. Huso, S. A. Fisher, M. K. Halushka, H. Kim, F. Qian, G. G. Germino and T. Watnick, *Cell reports*, 2014, **7**, 634-644.
23.A. San Martin, R. Foncea, F. R. Laurindo, R. Ebensperger, K. K. Griendling and F. Leighton, *Free radical biology & medicine*, 2007, **42**, 1671-1679.
24.Y. Gu, X. Chen, J. H. Lee, D. A. Monteiro, H. Wang and W. Y. Lee, *Acta biomaterialia*, 2012, **8**, 424-431.
25.A. Goldin, J. A. Beckman, A. M. Schmidt and M. A. Creager, *Circulation*, 2006, **114**, 597-605.
26.F. Wang, Y. L. Song, C. X. Li, D. H. Li, H. P. Zhang, A. J. Ma, X. Q. Xi, N. Zhang, B. G. Wang, Y. Wang and W. Zhou, *European journal of pharmacology*, 2010, **640**, 226-232.
27.G. K. Zou, Y. L. Song, W. Zhou, M. Yu, L. H. Liang, D. C. Sun, D. H. Li, Z. X. Deng and W. Z. Zhu, *Oral surgery, oral medicine, oral pathology and oral radiology*, 2012, **114**, 284-289.
28.X. Liu, N. Tan, Y. Zhou, H. Wei, S. Ren, F. Yu, H. Chen, C. Jia, G. Yang and Y. Song, *International journal of nanomedicine*, 2017, **12**, 7089-7101.
29.G. Ryan, A. Pandit and D. P. Apatsidis, *Biomaterials*, 2006, **27**, 2651-2670.
30.S. Arabnejad, R. Burnett Johnston, J. A. Pura, B. Singh, M. Tanzer and D. Pasini, *Acta biomaterialia*, 2016, **30**, 345-356.
31.K. Zhang, X. Tang, J. Zhang, W. Lu, X. Lin, Y. Zhang, B. Tian, H. Yang and H. He, *Journal of controlled release : official journal of the Controlled Release Society*, 2014, **183**, 77-86.
32.K. K. Chereddy, A. Lopes, S. Koussoroplis, V. Payen, C. Moia, H. Zhu, P. Sonveaux, P. Carmeliet, A. des Rieux, G. Vandermeulen and V. Preat, *Nanomedicine : nanotechnology, biology, and medicine*, 2015, **11**, 1975-1984.
33.S. Rafii, J. M. Butler and B. S. Ding, *Nature*, 2016, **529**, 316-325.
34.A. P. Kusumbe, S. K. Ramasamy and R. H. Adams, *Nature*, 2014, **507**, 323-328.
35.M. Grellier, L. Bordenave and J. Amedee, *Trends in biotechnology*, 2009, **27**, 562-571.
36.D. P. Herzog, E. Dohle, I. Bischoff and C. J. Kirkpatrick, *BioMed research international*, 2014, **2014**, 320123.
37.G. X. Ruan and A. Kazlauskas, *The Journal of biological chemistry*, 2013, **288**, 21161-21172.
38.M. Sjostrand, A. Holmang, L. Strindberg and P. Lonnroth, *American journal of physiology. Endocrinology and metabolism*, 2000, **279**, E1097-1103.
39.F. Meyer, J. Wardale, S. Best, R. Cameron, N. Rushton and R. Brooks, *Journal of orthopaedic research : official publication of the Orthopaedic Research Society*, 2012, **30**, 864-871.
40.T. Shoji, H. Koyama, T. Morioka, S. Tanaka, A. Kizu, K. Motoyama, K. Mori, S. Fukumoto, A. Shioi, N. Shimogaito, M. Takeuchi, Y. Yamamoto, H. Yonekura, H. Yamamoto and Y. Nishizawa, *Diabetes*, 2006, **55**, 2245-2255.
41.A. W. Stitt, C. McGoldrick, A. Rice-McCaldin, D. R. McCance, J. V. Glenn, D. K. Hsu, F. T. Liu, S. R. Thorpe and T. A. Gardiner, *Diabetes*, 2005, **54**, 785-794.
42.M. Yamamoto and T. Sugimoto, *Current osteoporosis reports*, 2016, **14**, 320-326.
43.Y. Hamada, S. Kitazawa, R. Kitazawa, K. Kono, S. Goto, H. Komaba, H. Fujii, Y. Yamamoto, H. Yamamoto, M. Usami and M. Fukagawa, *Endocrine*, 2010, **38**, 369-376.
44.N. Napoli, M. Chandran, D. D. Pierroz, B. Abrahamsen, A. V. Schwartz, S. L. Ferrari, I. O. F. Bone and G. Diabetes Working, *Nature reviews. Endocrinology*, 2017, **13**, 208-219.
45.L. Karim and M. L. Bouxsein, *Bone*, 2016, **82**, 21-27.

View Article Online
DOI: 10.1039/C7TB03247A

Table 1. Primers used in qPCR.

Gene	Forward primer sequence (5'-3')	Reverse primer sequence (5'-3')
EMCN	GCACCAAAAACATCACGGAGA	TGGTGGTGAAGTGTTAATCTTGG
PECAM-1	ATAAACGGAACAGCGCCCAT	ATCCACTGGGGCTATCACCT
VEGF-A	TCACCATGCAGATTATGCGGA	AGCGCTCCAGGATTTATACCG
TGF-B1	ACAATTCCTGGCGCTACCTC	CGGAACTGAACCCGTTGATG
RUNX2	GACAACGCACCAATGTGGA	CTACCACCTTGAAGCACGGG
Osterix	TTATCCCCCAGCTCTCTCCA	AAATTTACTGCACGCCGCTG
β-actin	GGACTATGACTTAGTTGCGTTAC	TTTGCATTACATAATTTACACGA

View Article Online
DOI: 10.1039/C7TB03247A

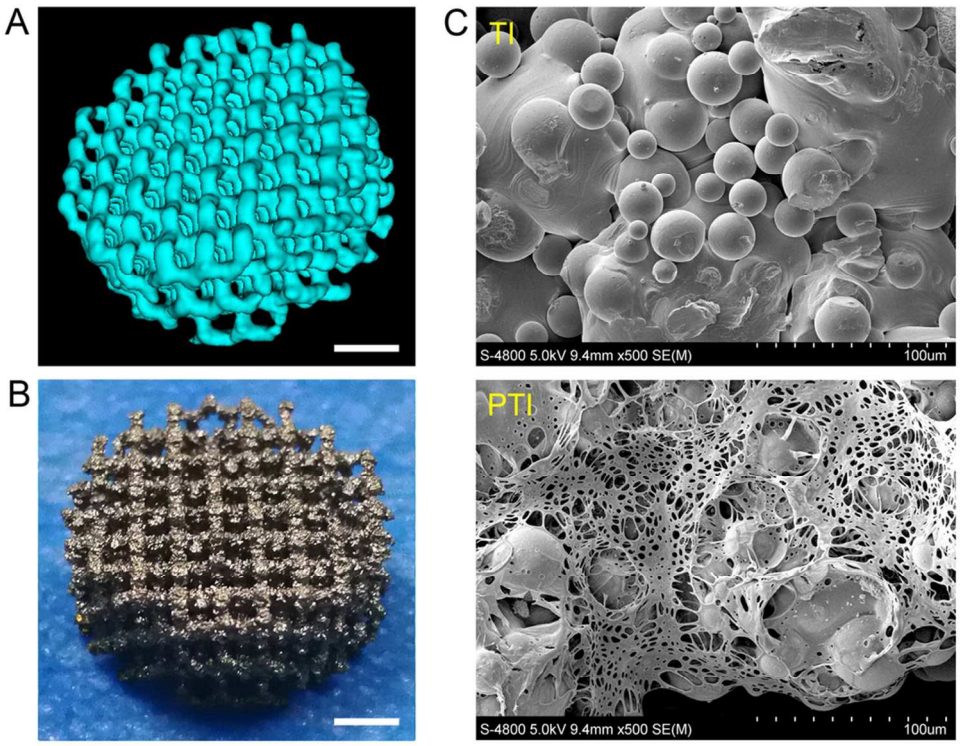

Fig. 1 Characterization of 3D-printed porous titanium implant (TI). (A) Micro-CT reconstruction of the spatial structure. (B) Gross view. (C) Scanning electron micrograph (SEM) micrographs showing the surface structures of titanium implants (TI) with and without reticular PLGA coating. Scale bar: 2 mm in (A) and (B).

47x37mm (600 x 600 DPI)

View Article Online
DOI: 10.1039/C7TB03247A

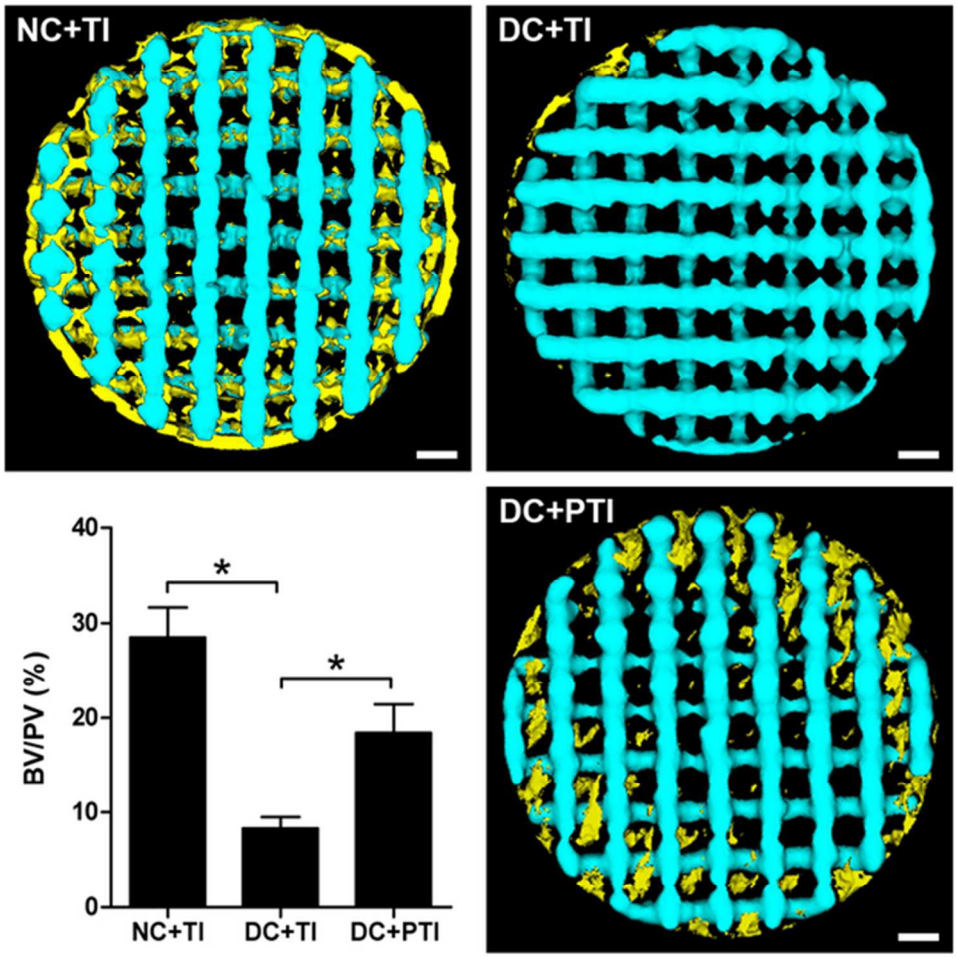

Fig. 2 Micro-CT analysis of the implant osseointegration 12 weeks after implantation. 3D reconstruction images of new bone ingrowth within the implants as sections toward the very center of the implants in terms of the z-dimension. Cyan as implant and yellow as bone. Scale bar: 1 mm. Quantitative analysis of the bone ingrowth within implant pores was exhibited as the percentage of bone volume to pore volume (BV/PV). TI, titanium implant; NM, normal milieu; DM, diabetic milieu. * $p < 0.05$.

27x28mm (600 x 600 DPI)

View Article Online
DOI: 10.1039/C7TB03247A

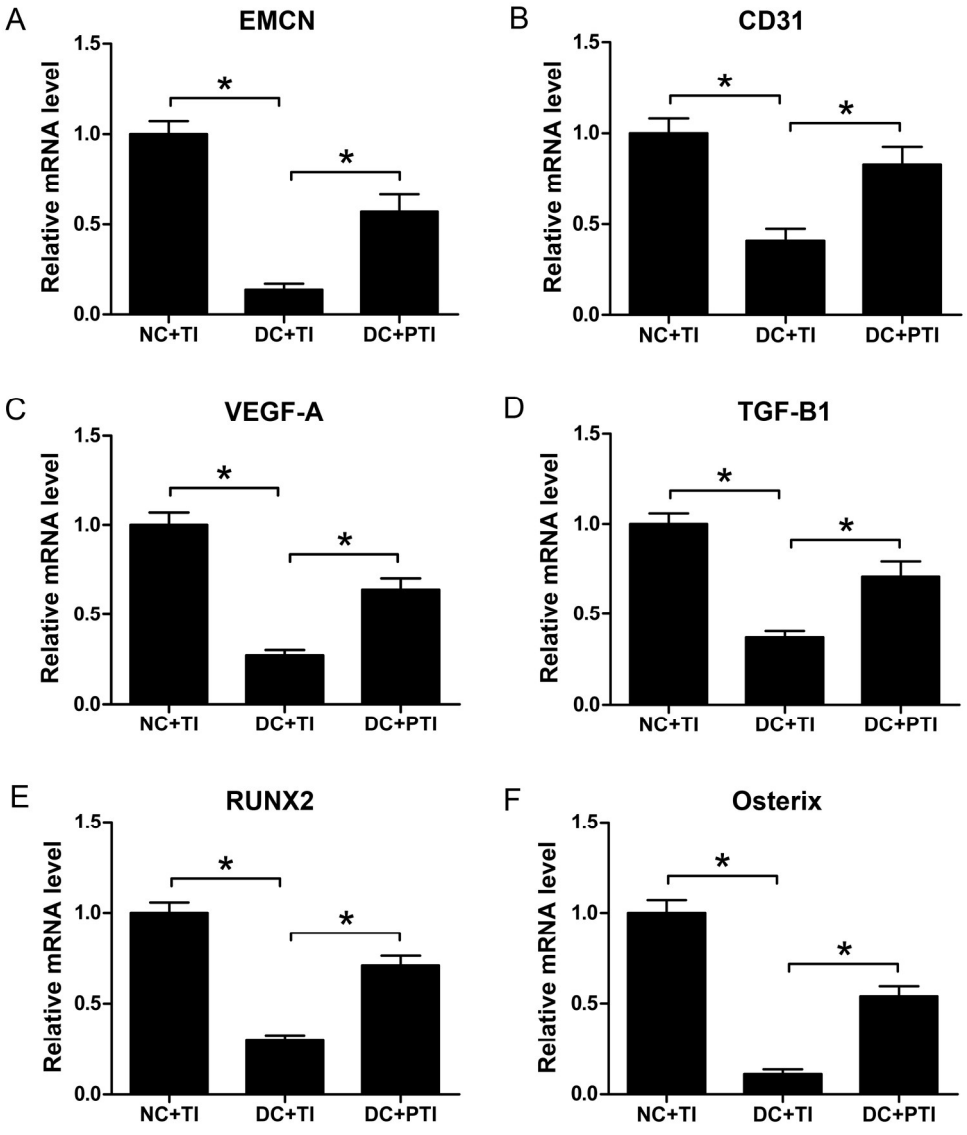

Fig. 3 Expression levels of molecules in the bone tissue around TI 4 weeks after implantation. qPCR analysis of the mRNA levels of the markers of VEC (EMCN and CD31), representative crucial cytokines for both angiogenesis and osteogenesis (VEGF-A and TGF-B1) as well as key genes in osteogenic cells during osteogenesis (RUNX2 and Osterix). * $p < 0.05$.

94x111mm (600 x 600 DPI)

View Article Online
DOI: 10.1039/C7TB03247A

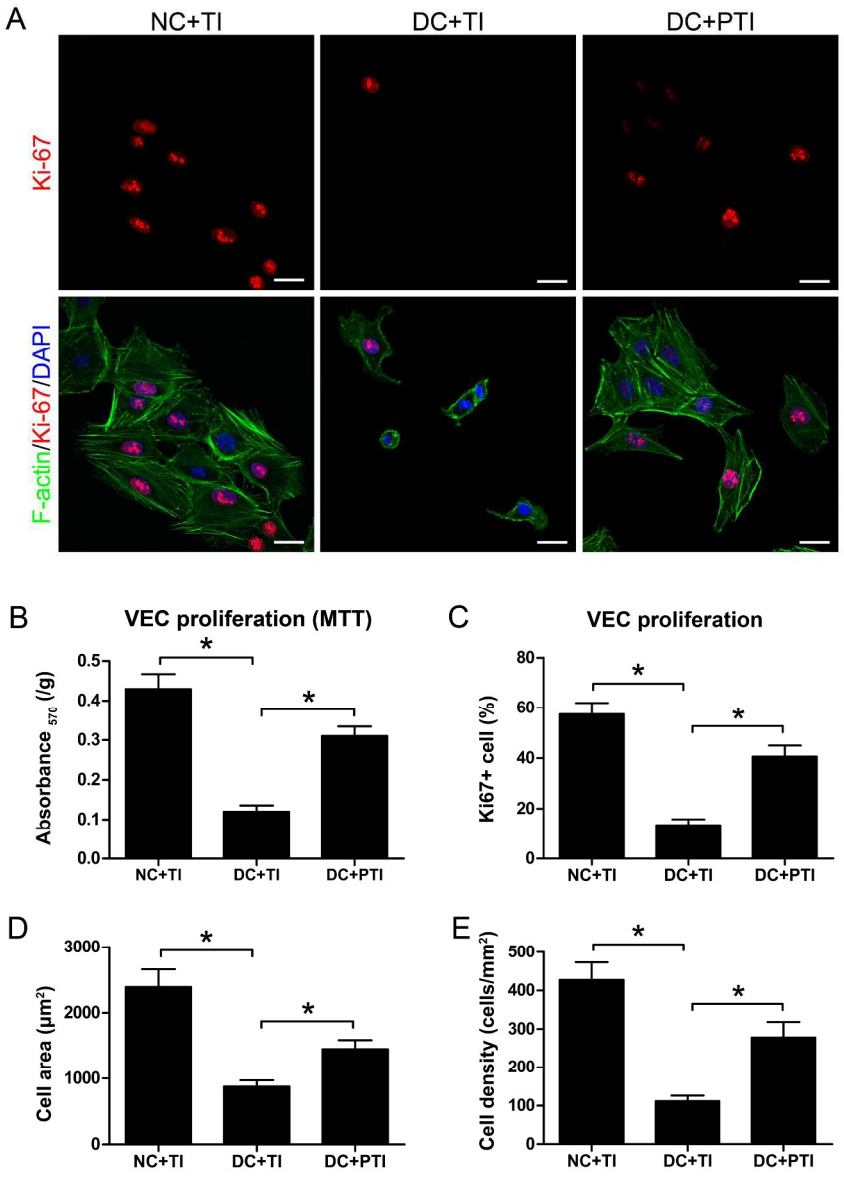

Fig. 4 Proliferation and adhesion of VEC after 7 days of incubation on different implants in NM and DM. (A) Representative images show cell proliferation marker (Ki67, red) and cell adhesion. The actin filaments (green) of VEC were stained with Alexa Fluor® 488 Phalloidin and cell nuclei (blue) were stained with DAPI. Proliferation of VEC was determined by colorimetric MTT assay (B) and the percentage of Ki-67+ cells (C). Cell adhesion was quantified with cell spreading area (D) and cell density (E). * $p < 0.05$.

139x190mm (600 x 600 DPI)

View Article Online
DOI: 10.1039/C7TB03247A

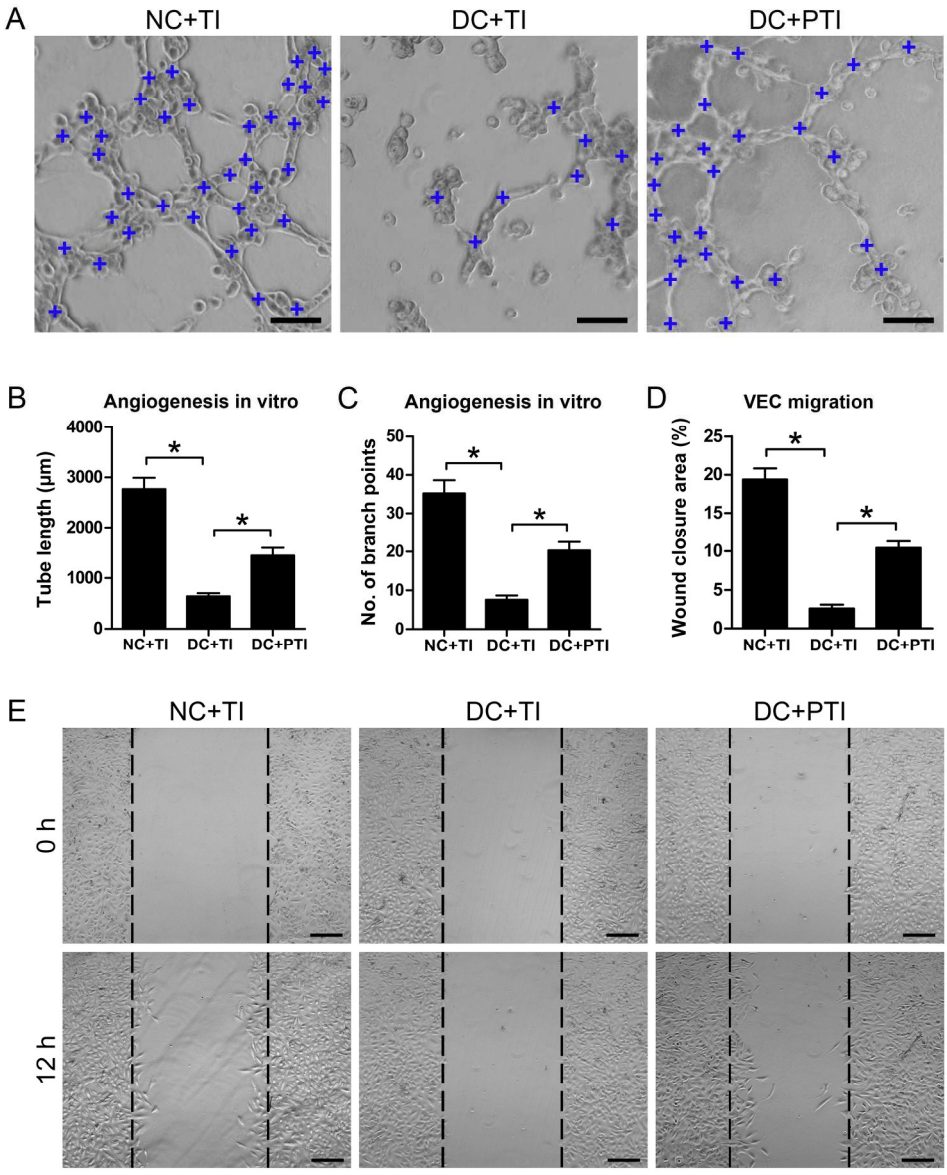

Fig. 5 Angiogenesis in vitro and cell migration of VEC after incubation under different conditions for 7 days. (A) Representative images in tube formation assay show the angiogenesis in vitro. Blue plus signs label the branch points of tubes. Quantitative analysis of cumulative tube length (B) and branch points (C) per microscopic field. (D) Quantification of cell migration with the percentage of wound closure area calculated by subtracting the area of the wound at 12 h from those at 0 h. (E) Representative images from wound-healing assay show the migration of VEC. Confluent monolayers were photographed at 0 h and 12 h after wounding. Dashed lines indicate the border of the wound at 0 h. Scale bar: 100 μm in (A) and 200 μm in (E). * $p < 0.05$.

98x121mm (600 x 600 DPI)

View Article Online
DOI: 10.1039/C7TB03247A

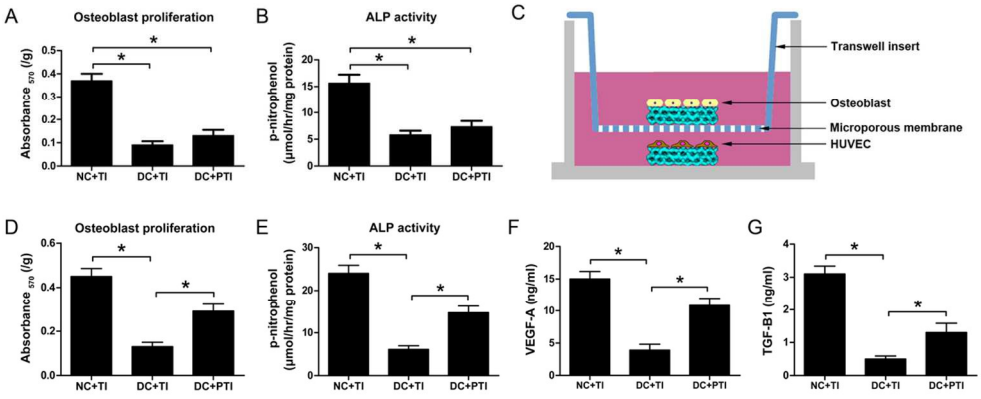

Fig. 6 Behaviors of osteoblasts after 7 days of incubation on implant surface. The proliferation (A) and ALP activity (B) of osteoblasts when they were monocultured on different implants. (C) Schematic diagram shows the coculture of VEC and osteoblasts on implants in Transwell system. The proliferation (D) and osteogenic differentiation (E) of osteoblasts as well as the levels of VEGF-A and TGF-B1 in the culture supernatant in coculture. * $p < 0.05$.

57x22mm (600 x 600 DPI)

View Article Online
DOI: 10.1039/C7TB03247A

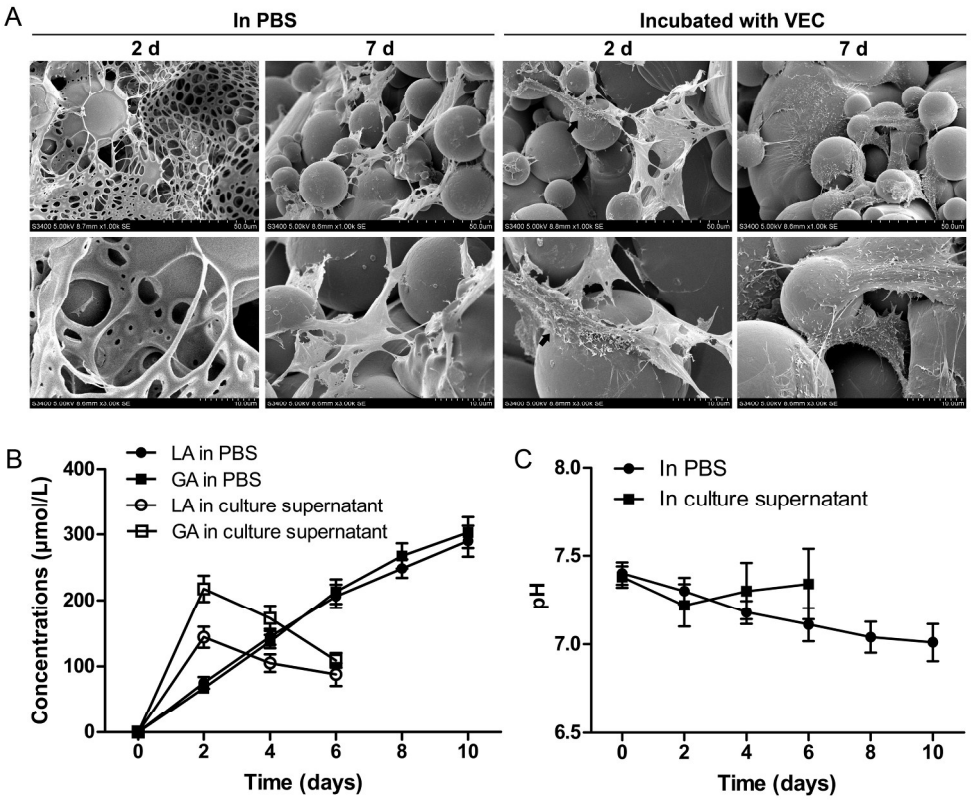

Fig. 7 Evaluation of the degradation of PLGA coating. (A) SEM images show the implant surfaces under different conditions at day 2 and 7. Black arrow indicates a VEC touching the squamaceous residue of PLGA coating. (B) The concentrations of the two degradation products, lactic acid (LA) and glycolic acid (GA), in PBS and in culture supernatant when PLGA-coated implants were incubated with VEC in NM. (C) The changes of pH in the media with the degradation of PLGA coating.

117x96mm (600 x 600 DPI)

View Article Online
DOI: 10.1039/C7TB03247A

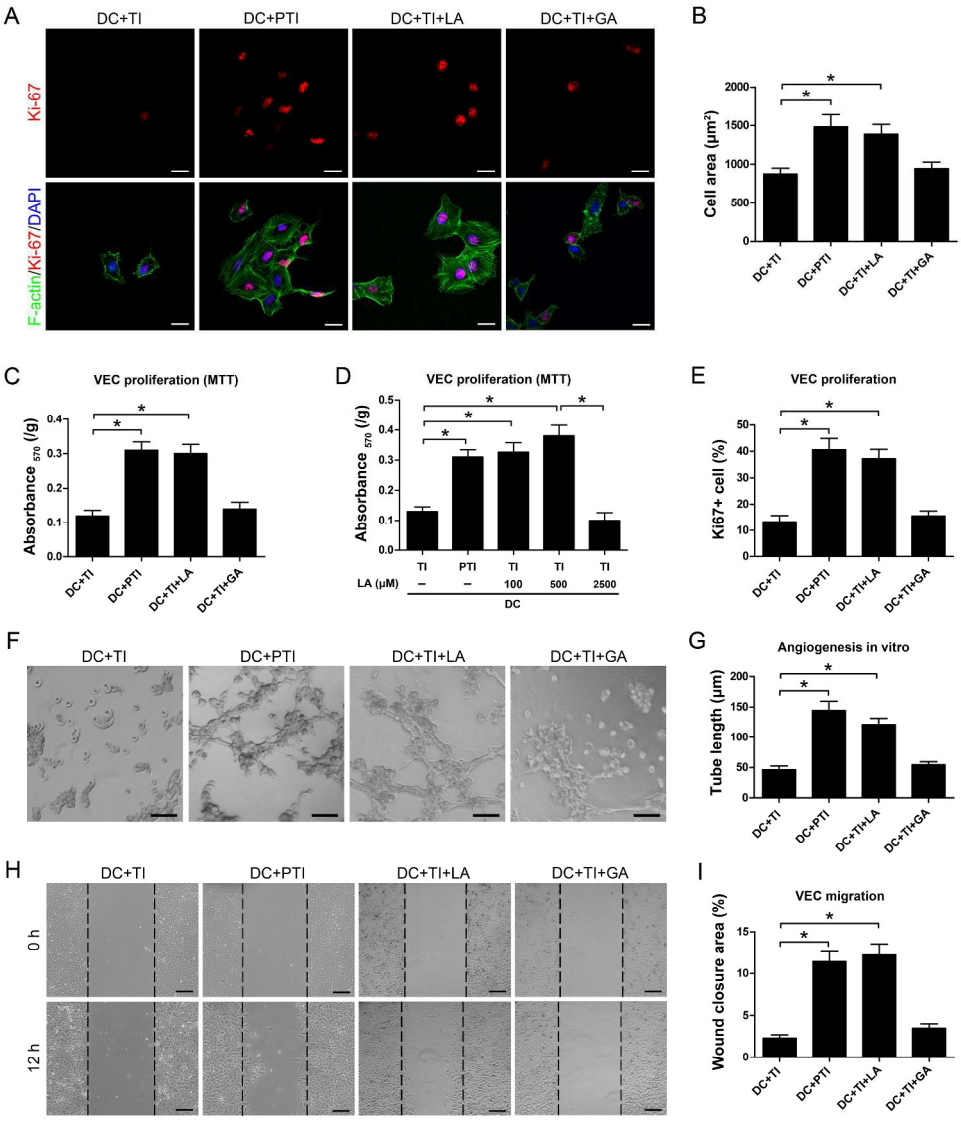

Fig. 8 The effects of the two degradation products of PLGA on VEC after 7 days of incubation on implants in DM. (A) Representative images show cell proliferation marker (Ki-67, red) and cell adhesion. The actin filaments (green) of VEC were stained with Alexa Fluor® 488 Phalloidin and cell nuclei (blue) were stained with DAPI. (B) Quantification of cell adhesion by cell spreading area. Proliferation of VEC was determined by colorimetric MTT assay (C and D) and the percentage of Ki-67+ cells (E). Representative images in tube formation assay (F) and quantitative analysis of cumulative tube length per microscopic field (G). (H) Representative images in wound-healing assay show the migration of VEC from 0 h to 12 h after wounding. Dashed lines indicate the border of the wounds at 0 h. (I) Quantification of VEC migration with the percentage of wound closure area calculated by comparing the wound area at 12 h to those at 0 h. Scale bar: 25 μm in (A), 100 μm in (F) and 200 μm in (H). * $p < 0.05$.

159x187mm (600 x 600 DPI)

View Article Online
DOI: 10.1039/C7TB03247A

View Article Online
DOI: 10.1039/C7TB03247A

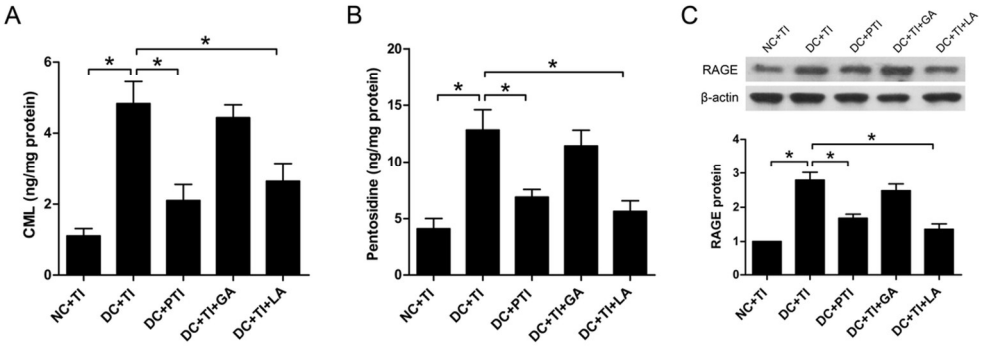

Fig. 9 The effects of PLGA coating and its degradation products on the advanced glycation end products (AGEs) and receptor for AGE (RAGE) in VEC on implants. The levels of two representative AGEs, Nε-carboxymethyllysine (CML, A) and pentosidine (B), in VEC were determined by ELISA assay after 7 days of incubation. (C) Western blot analysis of the protein levels of RAGE in the VEC in different groups. * $p < 0.05$.

52x18mm (600 x 600 DPI)

View Article Online
DOI: 10.1039/C7TB03247A

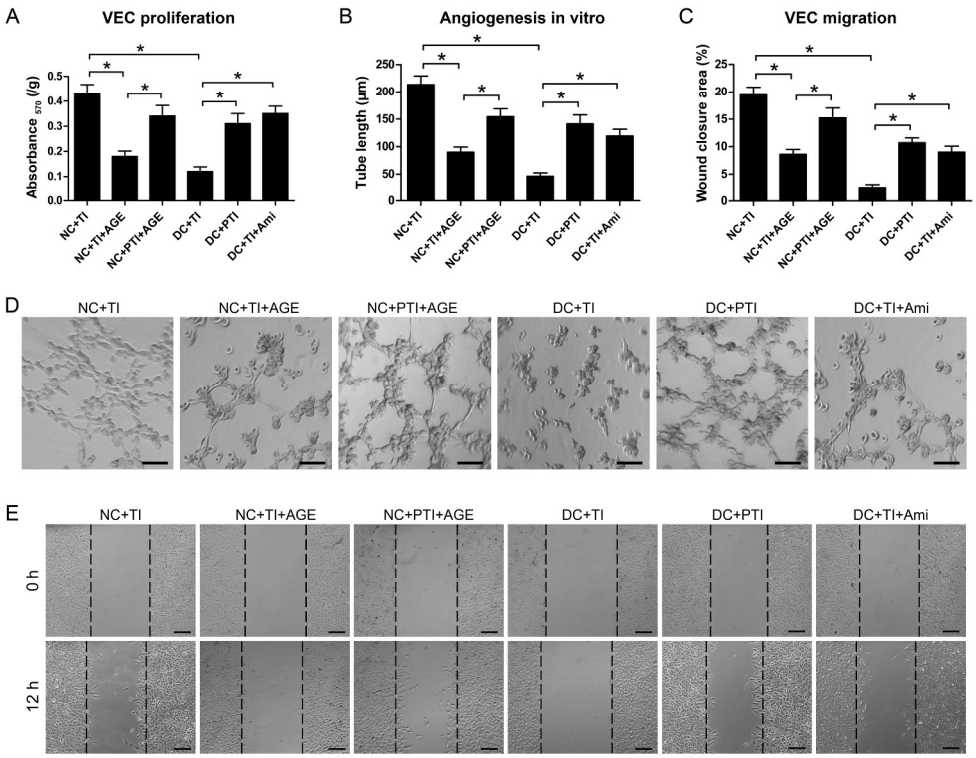

Fig. 10 The effects of PLGA coating on VEC were related to inhibiting the DM-induced up-regulation of the formation and effects of AGE. Experiments were conducted 7 days after incubation. (A) Proliferation of the VEC on implant surface. Representative tube formation assay images (D) and quantitative analysis of cumulative tube length per microscopic field (B) show the angiogenesis in vitro. (C) Quantification of VEC migration with the percentage of wound closure area calculated by comparing the wound area at 12 h to those at 0 h. (E) Representative images in wound-healing assay show the migration of EC from 0 h to 12 h. Ami (aminoguanidine), an inhibitor for AGEs formation. * $p < 0.05$.

117x91mm (600 x 600 DPI)

View Article Online
DOI: 10.1039/C7TB03247A

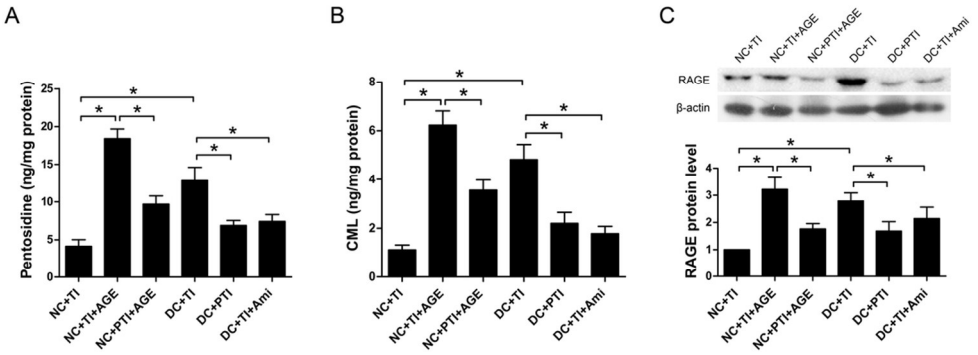

Fig. 11 The levels of AGEs and RAGE in VEC on implants after 7 days of incubation under different conditions. The CML (A) and pentosidine (B) in VEC were determined by ELISA assay. (C) Western blot analysis shows the protein levels of RAGE in VEC. Ami, aminoguanidine. * $p < 0.05$.

52x19mm (600 x 600 DPI)

View Article Online
DOI: 10.1039/C7TB03247A

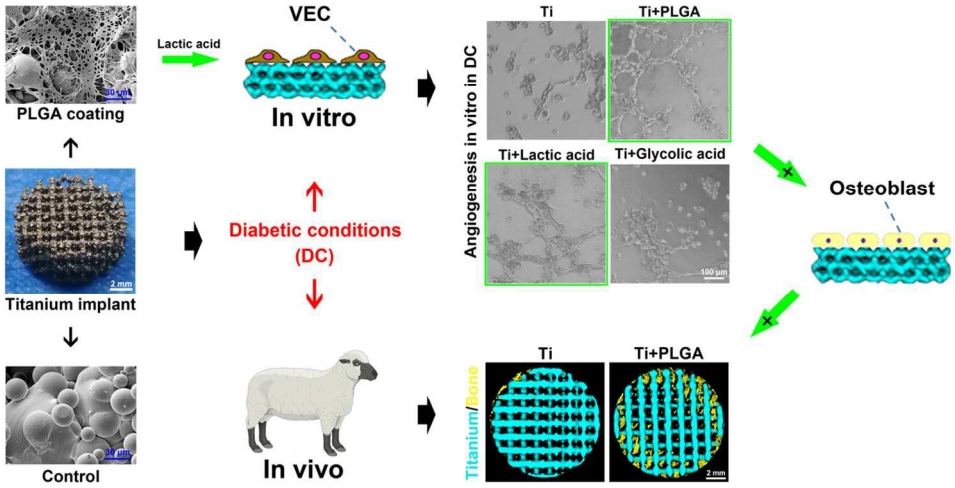

Graphical abstract: PLGA-coating on 3D-printed porous titanium implants promoted the angiogenesis and osteointegration at bone-implant interface in diabetes by releasing lactic acid.

117x61mm (300 x 300 DPI)